長崎大学工学研究科研究報告 第46 巻 第87 号 平成28 年7 月

UAV の現状と土木分野への応用

大坪俊太郎*,小川進*,日高悠広*,山田凱登*

Present State of UAV and Applications for Civil Engineering

by

Shuntaro OTSUBO*, Susumu OGAWA*, Haruhiro HIDAKA*, Gaito YAMADA*

UAV (Unmanned Aerial Vehicle) is effective for remote sensing and obtains high-resolution data at low cost rather than satellite images and aerial photos. However, there is a lot of remote sensing with satellite information, while there is a little remote sensing with UAV photogrammetry. Then the authors researched a present state of UAV and applications for civil engineering. The objectives of this study was to construct a 3D model, to make orthogonal photos, and to calculate NDVI, NDWI, chlorophyll-a, and turbidity distributions and water catchment areas from UAV photogrammetry. In this paper, the authors introduced 3 examples for remote sensing with UAV and discussed possibility of the future on UAV.

Key words: *UAV, NDVI, NDWI, 3D model, GIS*

1. Introduction

The modern remote sensing developed with the development of flights. In 1858, Tournachon, a balloonist took photographs in Paris from his balloon. In World War Ⅰ, aerial photography was the most advanced technology for military purpose. In the latter half of the twentieth century, it was possible to use remote sensing all over the world with satellites. Therefore, new aeronautical technology, UAV would develop remote sensing.

Also the authors made a 3D model from UAV photogrammetry with PhotoScan Professional. PhotoScan is a software that creates a 3D model with high resolution. In general, UAV has a wide-angle lens. A wide-angle lens makes lens distortion, but, PhotoScan corrects automatically the distortion with a correction algorithm. Moreover, PhotoScan allowed the authors to export orthogonal photos including GPS (Global positioning system) coordinates and DEM (Digital elevation model) data and also to calculate NDVI and another normalized vegetation index, NDWI.

Incidentally, the authors utilized data obtained from remote sensing as broadband data for GIS (Geographic Information System). The authors analyzed orthogonal photos with ArcGIS. ArcGIS enabled hydrological analysis, terrain analysis and hazard assessment.

2. Methods

2.1 Photographing methods with UAV

The authors utilized Phantom 3.0 Professional in this research. The authors used two filters, IR72 and IR90 to calculate NDVI and NDWI. The authors flew UAV with two filters twice more. Finally, a list of bands in this study is shown in Table 1.

Table 1　List of bands

Band	Wave length(nm)	Electric Magnetic Wave
1	450-520	Blue
2	520-600	Green
3	630-690	Red
4	760-900	Near Infrared
5	900-	Short Infrared

2.2 3D modeling with PhotoScan

The authors constructed a high-density cloud from UAV photogrammetry and GPS (Global Positioning System)

平成 28 年 6 月 28 日受付

＊ 長崎大学工学研究科社会環境デザイン工学コース

coordinates with Agisoft, PhotoScan Professional. Furthermore, constructing meshes and textures made a 3D model. Also the authors corrected lens distortion with the correction algorithm of lens distortion that Brown presented in PhotoScan.

2.3 Methods for orthogonal photos with PhotoScan

The authors made orthogonal photos from a 3D model with Agisoft, PhotoScan Professional. Furthermore, the authors made orthogonal photos which had 3D data by exporting in TIFF file format.

2.4 Calculation of NDVI and NDWI with Photoshop

The authors calculated NDVI with Adobe, Photoshop CS6 by subtracting orthogonal photos in Band 3 from orthogonal photos in Band 4 at the same position. In the same way, the authors calculated NDWI by subtracting orthogonal photos in Band 3 from orthogonal photos in Band 5. NDVI and NDWI are shown as next.

$$\mathrm{NDVI} = \frac{Band4 - Band3}{Band4 + Band3} \quad (1)$$

$$\mathrm{NDWI} = \frac{Band3 - Band5}{Band3 + Band5} \quad (2)$$

2.5 Calculation of chlorophyll-a and turbidity with PhotoScan

The authors calculated chlorophyll-a and turbidity distributions with a raster operation from UAV orthogonal photos with Agisoft, PhotoScan Professional.

2.6 Calculation of pH with PhotoScan

The authors analyzed bands and pH which the authors measured at 7 locations with a data analysis tool in Microsoft, Excel 2016. Then the authors calculated relation between pH and bands. The authors calculated quantitative pH distributions with a raster operation from UAV orthogonal photos with Agisoft, PhotoScan Professional.

2.7 Calculation of catchment with ArcGIS

The authors smoothed surfaces from DEM (Digital Elevation Model) in a 3D model with ESRI, ArcGIS. Furthermore, the authors constructed flow direction raster and cumulative-flow-rate value raster from DEM (Digital Elevation Model). Finally, the authors calculated catchments with flow direction raster and cumulative-flow-rate value raster with ArcGIS.

3. Results and Discussion

The authors curried out experiments for remote sensing with UAV at 3 locations, Onigi village in Nagasaki prefecture, damaged areas in Kumamoto prefecture, and the Isahaya bay in Nagasaki prefecture.

3.1 Results and discussion for Onigi Village

On 8 May 2016, the authors took aerial photos with Phantom 3.0 at Onigi village, Hasami town in Nagasaki prefecture. The objectives of this field work were to make a 3D model and orthogonal photos, to estimate NDVI, NDWI, and temperature distributions, and also to calculate catchments.

Fig.1 shows a 3D model of Onigi village. Moreover, the authors utilized 24 aerial photos with UAV from 60 meters of height above land. Constructing a 3D model makes DEM.

Fig.2 shows orthogonal photos in Onigi village. GIS is effective because these images include RGB data and also 3-dimentional information in a TIFF format.

Fig.3 shows NDVI distributions in Onigi Village. NDVI was high in paddy fields that have been abandoned and are no longer cultivated. NDVI was middle or low in rice terraces at Onigi village. The rice planting season is early in May at Onigi village. Therefore, the authors inferred that NDVI was higher in a place completed by rice seeding than in a place without rice seeding.

Figs.4(a), (b), and (c) show flow direction raster, flow rate value raster, and a catchment in Onigi village respectively.

It was impossible to infer a distribution of NDWI and temperatures in the experiment at Onigi village because aerial photos with IR90 filter was not clear. These photos did not enable to synthesize UAV photogrammetry with IR90. Additionally, Phantom 3.0 had faults that it was impossible to take a picture in manual setting and to adjust ISO, shutter speeds, and diaphragm values.

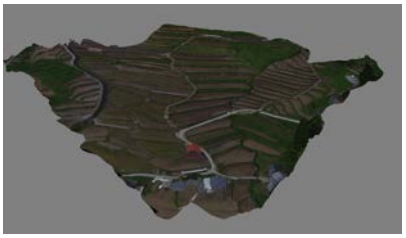

Fig.1 3D model at Onigi village

Fig.2　Orthogonal image at Onigi village

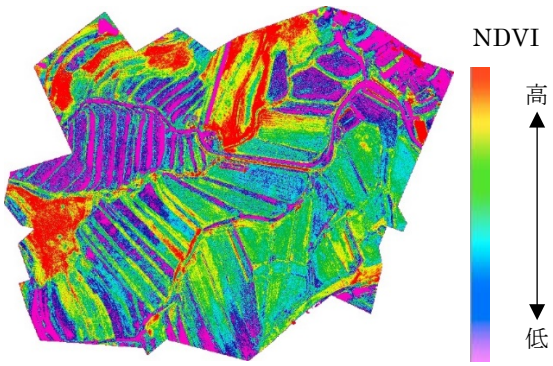

Fig.3　NDVI distribution map at Onigi village

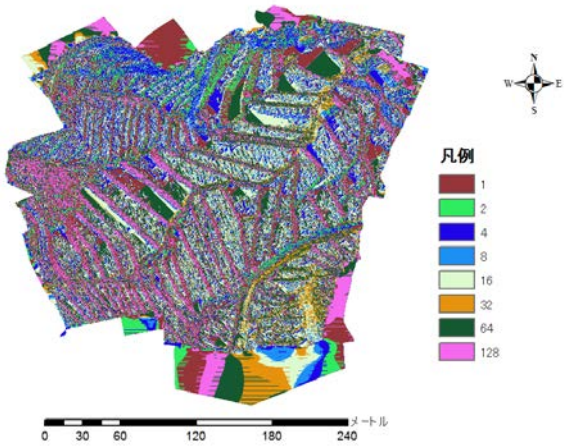

Fig.4(a)　Current directions at Onigi village

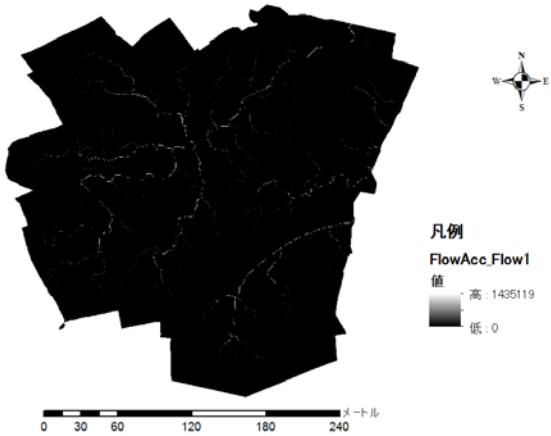

Fig.4(b)　Cumulative flows at Onigi village

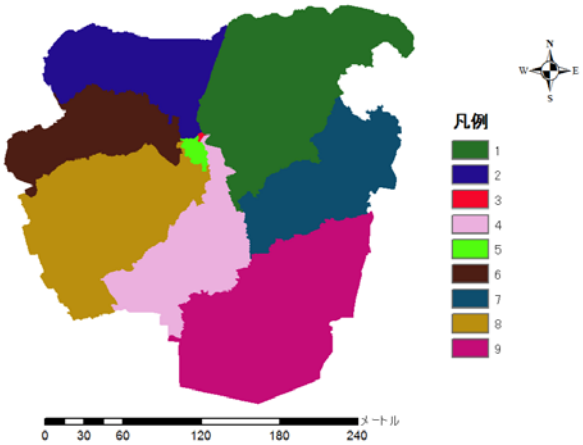

Fig.4(c)　Water catchment area at Onigi village

3.2 Results and discussion for Kumamoto

On 24 April 2016, the authors took aerial photos with Phantom 3.0 at Akitsukawa bridge in Mashiki town, Kumamoto prefecture. Additionally, on 28 May 2016, the authors took aerial photos with Phantom 4.0 at Aso Big Bridge in Cyoyo village, Kumamoto prefecture. The objectives of this field work were to make a 3D model and to grasp the damage situation.

Fig.5(a) shows a 3D model of Akitsukawa bridge. Fig.5(b) shows a DEM model of Akitsukawa bridge which the authors made from a 3D model. According to a 3D model, the authors found out that superstructures moved. The authors inferred that it resulted by deviating from bearing. Furthermore, according to DEM data, the authors found out that there was no level difference at moved superstructures. Therefore, the authors concluded

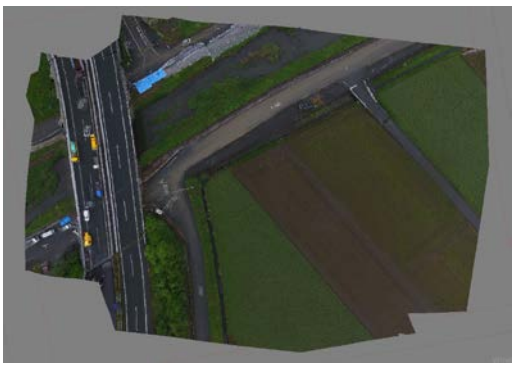

Fig.5(a)　3D model at Akitsukawa bridge

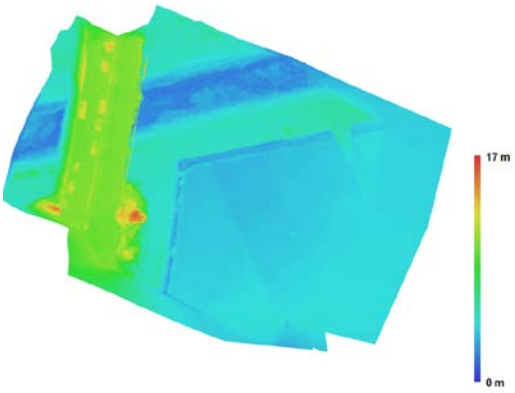

Fig.5(b)　DEM at Akitsukawa bridge

that bearing was not broken.

Fig.6(a) shows orthogonal image of Aso Big Bridge. Fig.6(b) shows a DEM model of Aso Big Bridge. Additionally, DEM images showed contours, directions of dips, and shaded-relief maps with ArcGIS. Fig.6(c) shows contours of Aso Big Bridge. Fig.6(d) shows directions of dips of Aso Big Bridge. Fig.6(e) shows a shaded-relief map at Aso Big Bridge. According to Figs.6 (c), (d), and (e), the authors found that there was steep slope collapse in the east and southwest. Thus, remote sensing with UAV showed the destruction of bridges and slope collapse. Additionally, when the authors took a picture with UAV at Aso Big Bridge, it rained about 1 mm/h. But it was possible to fly UAV in a little rain.

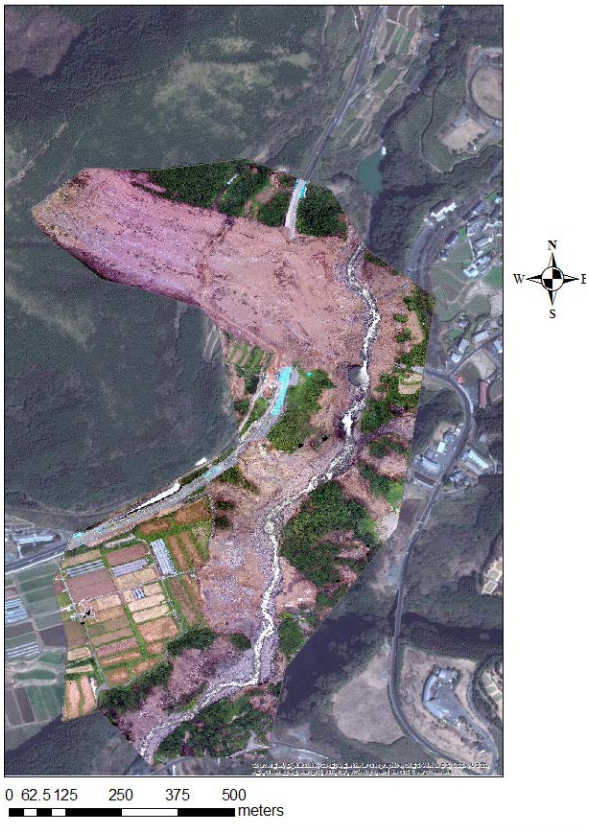

Fig.6(a) Orthogonal image at Aso Big Bridge

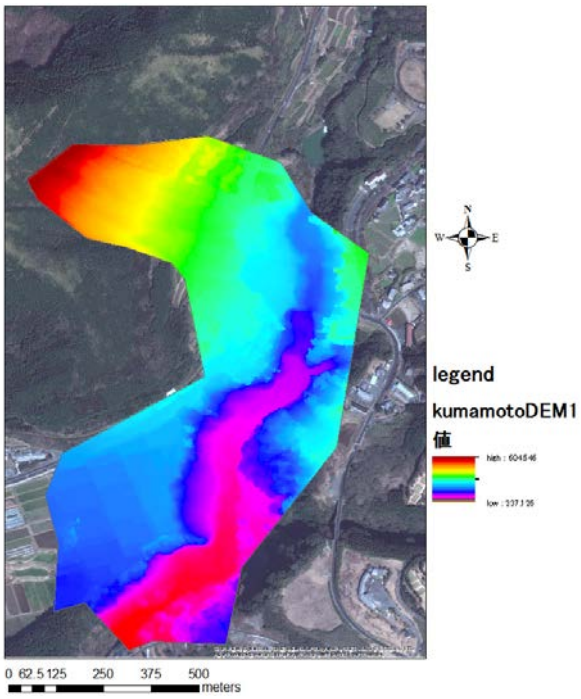

Fig.6(b) DEM image at Aso big bridge

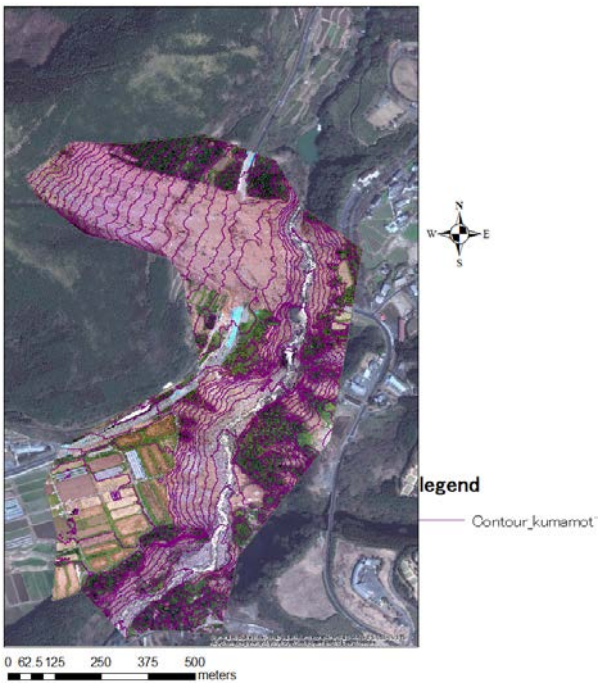

Fig.6(c) Contours at Aso Big Bridge(10m)

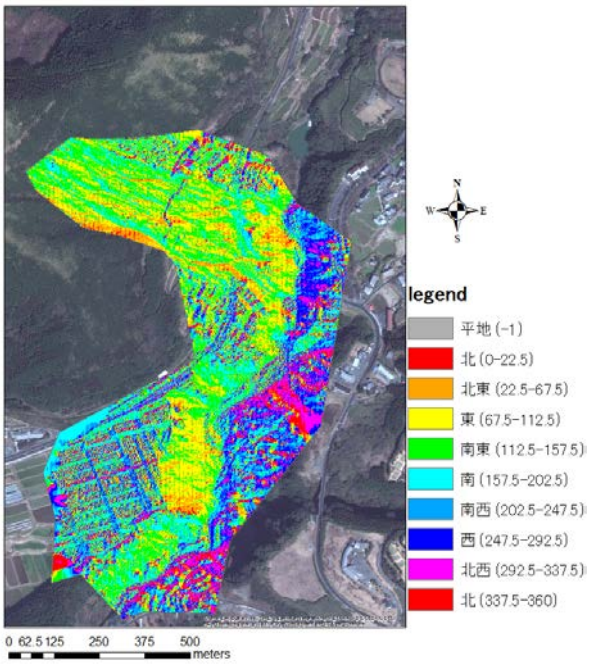

Fig.6(d) Directions of dips at Aso Big Bridge

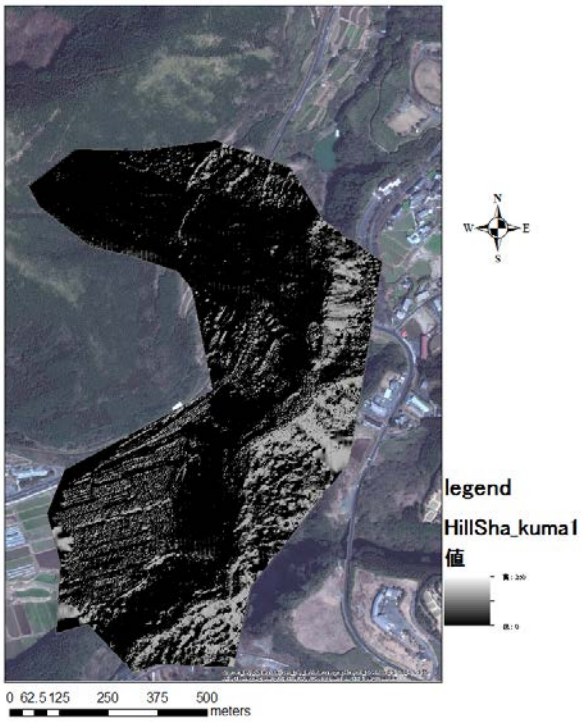

Fig.6(e) Shaded-relief map at Aso Choyo bridge

3.3 Results and discussion for Isahaya

On 7 May, 2016, the authors took aerial photos with Phantom 3.0 in the Isahaya bay in Nagasaki prefecture. The objectives of this field work were to make chlorophyll-a, turbidity and pH distributions.

Fig.7(a) shows an orthogonal image of the Isahaya bay. Fig.7(b) shows a chlorophyll-a distribution in the Isahaya bay. Fig.7(c) shows a turbidity distribution in the Isahaya bay.

The authors utilized UAV to take aerial photos on land at a distance of 500 meters. The authors constructed a 3D model in the Isahaya bay to make orthogonal photos. However, it was impossible to make a 3D model from only water surface pictures. On the other hand, it was possible to make a 3D model from water and land surface pictures. The authors concluded that it was caused mainly by sequential wave change.

According to Figs.7(b) and (c), chlorophyll-a and turbidity were low in the river, while chlorophyll-a and turbidity were high in the bay. Moreover, in the east bay, chlorophyll-a and turbidity were the highest because a sewage treatment plant named Korai Cleaning Center drained organic salts.

Fig.7(a) Orthogonal image in the Isahaya bay

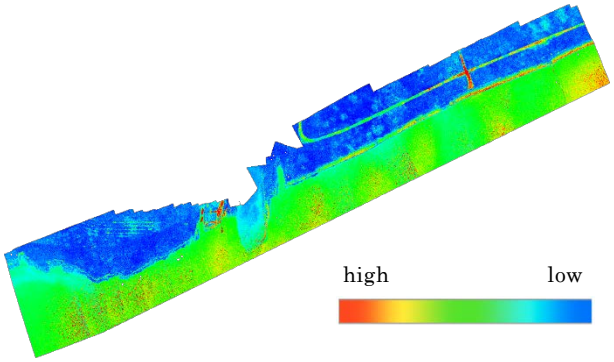

Fig.7(b) Chlorophyll-a distribution in the Isahaya bay

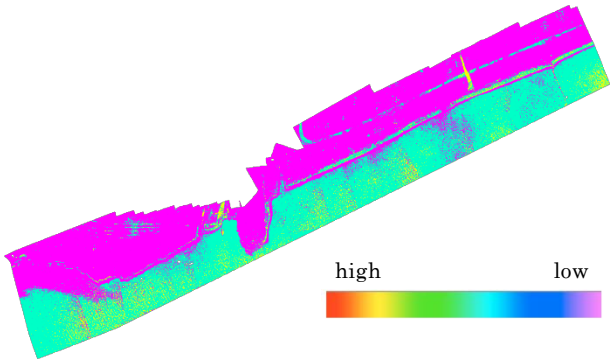

Fig.7(c) Turbidity distribution in the Isahaya bay

Fig.7(d) shows a pH distribution in the Isahaya bay. Table 2(a) shows bands and pH measured in each station in the Isahaya bay. Table 2(b) shows regression statistics. Table 2(c) shows regression analysis-results.

According to Table 2(b), the multiple correlation coefficient was 0.900. Thus, pH had relation among three bands. pH is shown as next (3).

$$pH = -0.012\ \ Band\ \ 1 + 0.048\ \ Band\ \ 2 - 0.012\ \ Band\ \ 3 + 7.405 \quad (3)$$

Regression equation (3) estimated pH as Fig.7(d). According to Fig.7(d), pH was low in the river, while pH was high in the bay. Chlorophyll- a was higher in the bay than the river.

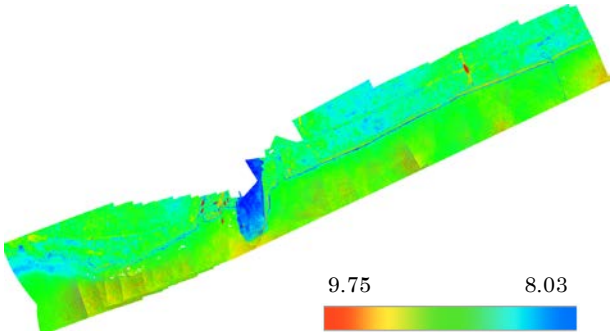

Fig.7(d) pH distribution in the Isahaya bay

Table 2(a) Bands and pH measured each station

state	pH	band1	band2	band3
1	8.762	56	56	56
2	8.750	45	45	35
7	8.762	32	46	48
8	8.832	52	50	50
9	8.757	51	50	50
11	8.100	28	30	38
12	9.000	49	50	51

Table 2(b) Multiple regression statistics

Items	Values
multiple correlation coefficient R	0.900
multiple determination coefficient R2	0.811
standard error of the mean	0.174
observation spots	7

Table 2(c) Results of regression analysis

values	coefficient	standard error	t	P Value	lower limit 95%	upper limit 95%
intercept	7.405	0.463	15.997	0.001	5.932	8.879
X value 1	-0.008	0.014	-0.592	0.595	-0.051	0.035
X value 2	0.048	0.022	2.168	0.119	-0.022	0.118
X value 3	-0.012	0.015	-0.804	0.480	-0.061	0.036

Therefore, because photosynthesis is more active in the bay, carbon dioxide is low and alkali is high.

4. Conclusions

The authors discussed a present state of UAV and applications for civil engineering. The objectives of this study was to construct a 3D model, to make orthogonal photos, and to calculate NDVI, NDWI, chlorophyll-a, and turbidity distributions, and water catchment areas from UAV photogrammetry. As a result, it was possible to calculate data in higher resolution than satellite data except NDWI. A camera of UAV had low performance. It is effective for remote sensing with UAV in any climates

except heavy rains. Above all, the authors concluded that UAV would apply for many fields of civil engineering.

Moreover, it was impossible to fly UAV in a place with an electric line in high voltage. There was also a danger for bird strikes.

Acknowledgements

The authors greatly appreciate for much cooperation by Profs. Yoichi Imamura and Seiji Suzuki, and Mr. Tran Thanh Dan.

References

1) Hirohumi Chikatsu, Akihiko Kodaka, Shuji Yanagi, Masaru Yokoyama: Performance assessment of 3D modeling software in UAV photogrammetry measurement, Journal of the Japan Society of Photogrammetry and Remote Sensing, pp117-127, 2016.
2) Akiyuki Kawasaki, Satoshi Yoshida: Graphic illustration of ArcGIS, part2: Step-up for practical GIS, Kokon Shoin Publisher, pp42-53, 2013.